# Relativistic many-body calculations of excitation energies and oscillator strengths in Ni-like ions

U. I. Safronova and W. R. Johnson
*Department of Physics, University of Notre Dame, Notre Dame, Indiana 46556*

J. R. Albritton
*Lawrence Livermore National Laboratory, P.O. Box 808, Livermore, California 94551*

(Received 8 May 2000; published 11 October 2000)

Excitation energies for $3l$-$4l'$ particle-hole states of Ni-like ions are determined to second order in relativistic many body perturbation theory. The calculations start from a closed-shell Dirac-Fock potential, and include second-order Coulomb and Breit-Coulomb interactions. Retarded electric-dipole matrix elements (in length and velocity forms) are calculated in second order for transitions from excited $3l$-$4l'$ states to the closed-shell ground state. Wavelengths for 3-4 and 4-4 transitions are compared with experimental data, and with other high-precision calculations. Trends of oscillator strengths as functions of nuclear charge $Z$ are shown graphically for selected transitions.

PACS number(s): 32.30.Rj, 32.70.Cs, 31.25.Jf, 31.15.Md

## I. INTRODUCTION

This is the second in a series of relativistic many-body perturbation theory (MBPT) studies of atomic characteristics of particle-hole excitations of closed-shell ions. In the first of these studies, energies [1–3] and oscillator strengths [4] in Ne-like ions were considered by Avgoustoglou and coworkers.

The second-order MBPT calculations for Ni-like ions start from a $1s^22s^22p^63s^23p^63d^{10}$ Dirac-Fock potential. We consider all possible $3l$ holes and $4l$ particles leading to 56 odd-parity and 50 even-parity $3l^{-1}4l'(J)$ states. We calculate energies of the 106 states for 18 representative ions with nuclear charge $Z$ ranging from 47 to 82. For odd-parity states with $J=1$, we extend our calculations of energies to $Z$ from 47 to 92, and line strengths to $Z$ from 32 to 100.

The Ni-isoelectronic sequence has been studied extensively, especially in recent years, in connection with x-ray lasers. The lasing action occurs because the $3d^{-1}4d$ levels are metastable to radiative decay to the Ni-like ground state; the transitions to the ground state from the lower $3d^{-1}4p$ levels are of course radiatively allowed. Ni-like x-ray lasers were first demonstrated in 1987 in a laser produced plasma of Eu, and later in laser-produced plasmas of Ta, W, and Au (see Refs. [5,6], and references therein). Accurate knowledge of the lasing wavelengths is essential for applications to laboratory x-ray lasers. Wavelength of $3d^94d^1S_0$-$3d^94p^1P_1$ x-ray lines in several low-$Z$ Ni-like ions ranging from Y ($Z=39$) to Cd ($Z=48$) were measured recently by Li *et al.* [7]. Measurements for two lasing lines: $3d_{3/2}4d_{3/2}(0)$-$3d_{5/2}4p_{3/2}(1)$ and $3d_{3/2}4d_{3/2}(0)$-$3d_{5/2}4p_{1/2}(1)$ in ions ranging from Nd ($Z=60$) to Ta ($Z=73$) were reported by Daido *et al.* in Ref. [8]. It should be noted that neither $LS$- nor $jj$-coupling schemes described these states properly; this is why different designations are used for these states in Refs. [7] and [8]. Lasing on the Ni-like $3d^94f^1P_1$–$3d^94d^1P_1$ x-ray line in Zr ($Z=40$), Nb ($Z=41$), and Mo ($Z=42$) was reported recently by Nilsen *et al.* in Ref. [9]. Measured wavelengths were presented for these ions as well as predicted values for ions from $Z=36$ to 54. The predictions in Ref. [9] were made by fiting the differences between energies calculated with the multiconfiguration Dirac-Fock (MCDF) code, and experimentally determined energies for $Z=37$–$42$ to a straight line. A similar method was used for predicting lasing lines in Refs. [5] and [7]. Accurate theoretical values for two lasing lines: $3d_{3/2}4d_{3/2}(0)$-$3d_{5/2}4p_{3/2}(1)$ and $3d_{3/2}4d_{3/2}(0)$-$3d_{5/2}4p_{1/2}(1)$ in selected Ni-like ions with $Z$ from 60 to 73 were presented in Ref. [8], where it was shown that good agreement between theoretical and experimental wavelengths could be obtained by taking into account the $d$-correlation.

A detailed analysis of 3-4 transitions in the x-ray spectrum by laser produced plasmas of Ba ($Z=56$), La ($Z=57$), and Pr ($Z=59$) was reported recently by Doron *et al.* [10] and Zigler *et al.* [11]. Ab-initio calculations were performed in Ref. [10] using the RELAC relativistic computer code to identify $3d$-$nf$ ($n=4-8$), $3p$-$4s$, and $3p$-$4d$ transitions of Ni-like Ba. The same computer code was used by Busquet *et al.* [12] to identify x-ray spectral lines emitted by a target of Au ($Z=79$). In Ref. [12], a detailed description of the RELAC code, which is based on a relativistic model potential, was given. The HULLAC package is also based on a relativistic model potential [13]. The $n=3$–$4$ transitions observed in x-ray spectra of Ni-like ions ($Ag^{19+}$-$Pb^{54+}$) were investigated theoretically by Quinet and Biémont [14], where the MCDF approach (Grant's code) was used to calculate wavelengths and oscillator strengths for the $3d$-$4p$, $3d$-$4f$, $3p$-$4s$, and $3p$-$4d$ electric-dipole transitions. The theoretical results in Ref. [14] were compared with all previous published experimental data obtained from x-ray spectra emitted by strongly ionized atoms, and generated by vacuum sparks, Tokamaks or high power lasers and the difference between theoretical and experimental values for the 3-4 transition were found to be about 0.5%.

There are fewer papers concerned with the analysis of the $4s$-$4p$ and $4p$-$4d$ transitions in Ni-like ions. Spectra of 4-4 transitions in a laser-produced plasma of Ni-like ions

 

($Ru^{16+}$-$Sn^{22+}$) were observed and analyzed by Churilov *et al.* in Ref. [15]. The analysis of these spectra was based on the theoretical prediction by Wyart [16]. The prediction of $4s$-$4p$ and $4p$-$4d$ transitions in Ni-like ions ($Mo^{14+}$-$Sn^{22+}$) in Ref. [16] was based on Slater-Condon-type calculations of $3d^9 4s$, $3d^9 4p$, and $3d^9 4d$ configurations. The radial parameters involved in the three configurations were determined by a generalized least-squares fit using all known levels in the sequence.

In the present paper, a relativistic MBPT is used to determine energies of $3l^{-1}4l'(J)$ states of Ni-like ions. Energies are calculated for the 56 odd-parity $3d^{-1}4p(J)$, $3d^{-1}4f(J)$, $3p^{-1}4s(J)$, $3p^{-1}4d(J)$, $3s^{-1}4p(J)$, and $3s^{-1}4f(J)$ excited states and the 50 even-parity $3d^{-1}4s(J)$, $3d^{-1}4d(J)$, $3p^{-1}4p(J)$, $3p^{-1}4f(J)$, $3s^{-1}4s(J)$, and $3s^{-1}4d(J)$ excited states for 18 representative Ni-like ions with $Z=47$–$82$. The energies of the 13 odd-parity states with $J=1$ are calculated for Ni-like ions with $Z=47$–$92$.

Relativistic MBPT is also used to determine reduced matrix elements and oscillator strengths for electric dipole transitions from the $3l^{-1}4l'(1)$ states to the $^1S_0$ ground state in Ni-like ions with nuclear charges $Z$ ranging from 32 to 100. Retarded $E1$ matrix elements are evaluated in both length and velocity forms. The MBPT calculations start from a nonlocal $1s^2 2s^2 2p^6 3s^2 3p^6 3d^{10}$ Dirac-Fock potential, and consequently give gauge-dependent transition matrix elements. Second-order correlation corrections compensate almost exactly for the gauge dependence of the first-order matrix elements, leading to corrected matrix elements that differ by less than 1% in length and velocity forms throughout the periodic system.

## II. METHOD

Details of the MBPT method were presented in Ref. [1] for a calculation of energies of particle-hole states, in Ref. [17] for calculation of energies of particle-particle states, and in Ref. [18] for calculation of radiative transition rates in two-particle states. Here we will present only the model space for Ni-like ions and the first- and second-order diagram contributions for particle-hole systems without repeating the detailed discussions given in Refs. [1], [17], and [18].

### A. Model space

For atoms with one hole in closed shells and one electron above closed shells, the model space is formed from particle-hole states of the type $a_v^+ a_a|0\rangle$, where $|0\rangle$ is the closed-shell $1s^2_{1/2}2s^2_{1/2}2p^2_{1/2}2p^4_{3/2}3s^2_{1/2}3p^2_{1/2}3p^4_{3/2}3d^4_{3/2}3d^6_{5/2}$ ground state. The single-particle indices $v$ range over states in the valence shell and the single-hole indices $a$ range over the closed core. For our study of low-lying states $3l^{-1}4l'$ states of Ni-like ions, values of $a$ are $3s_{1/2}$, $3p_{1/2}$, $3p_{3/2}$, $3d_{3/2}$, and $3d_{5/2}$, while values of $v$ are $4s_{1/2}$, $4p_{1/2}$, $4p_{3/2}$, $4d_{3/2}$, $4d_{5/2}$, $4f_{5/2}$, and $4f_{7/2}$. To obtain orthonormal model states, we consider the coupled states $\Phi_{JM}(av)$ defined by

$$\Phi_{JM}(av)=\sqrt{(2J+1)}\sum_{m_a m_v}(-1)^{j_v-m_v}\times\begin{pmatrix} j_v & J & j_a \\ -m_v & M & m_a\end{pmatrix}a^\dagger_{vm_v}a_{am_a}|0\rangle. \quad (2.1)$$

Combining the $n=3$ hole orbitals and the $n=4$ particle orbitals in nickel, we obtain 56 odd-parity states consisting of five $J=0$ states, 13 $J=1$ states, 15 $J=2$ states, 12 $J=3$ states, seven $J=4$ states, two $J=5$ states, and two $J=6$ states. Additionally, there are 50 even-parity states consisting of five $J=0$ states, 12 $J=1$ states, 14 $J=2$ states, 11 $J=3$ states, six $J=4$ states, one $J=5$ state, and one $J=6$ state. The distribution of the 116 states in the model space is summarized in Table I.

### B. Energy matrix

The first-order energy-matrix element for a particle-hole system $va(J)$ is

$$E^{(1)}[a'v'(J),av(J)]=\delta_{vv'}\delta_{aa'}(\epsilon_v-\epsilon_a)+\frac{1}{(2J+1)}\times(-1)^{j_v+j_a+J+1}Z_J(av'va'), \quad (2.2)$$

where $\epsilon_i$ is the eigenvalue of the Dirac-Hartree-Fock (DHF) equation for state $i$, and where

$$Z_J(abcd)=X_J(abcd)+\sum_k(2J+1)X_k(abdc)\times\begin{Bmatrix} j_a & j_c & J \\ j_b & j_d & k\end{Bmatrix}, \quad (2.3)$$

with

$$X_k(abcd)=\langle a||C_k||c\rangle\langle b||C_k||d\rangle R_k(abcd). \quad (2.4)$$

The quantities $C_k$ are normalized spherical harmonics and $R_k(abcd)$ are Slater integrals. The corresponding second-order energy matrix is

$$E^{(2)}[a'v'(J),av(J)]=\delta_{vv'}\delta_{aa'}(E^{(2)}_v+E^{(2)}_a)+\sum_{i=1,4}E^{R_i}[a'v'(J),av(J)]. \quad (2.5)$$

The second-order one-particle $E^{(2)}_v$ and one-hole $E^{(2)}_a$ contributions are defined by three terms: double sums, single sums, and a one-potential term. This later term contributes only to the Breit-Coulomb correction. The second-order contribution for hole state $a$ ($E^{(2)}_a$) is

TABLE I. Possible hole-particle states in the $3lj4l'j'$ complex; $jj$-coupling scheme.

Odd-parity states

| $J=0$ | $J=1$ | $J=2$ | $J=3$ | $J=4$-6 |
|---|---|---|---|---|
| $3d_{3/2}4p_{3/2}(0)$ | $3d_{5/2}4p_{3/2}(1)$ | $3d_{5/2}4p_{1/2}(2)$ | $3d_{5/2}4p_{1/2}(3)$ | $3d_{5/2}4p_{3/2}(4)$ |
| $3d_{5/2}4f_{5/2}(0)$ | $3d_{3/2}4p_{1/2}(1)$ | $3d_{5/2}4p_{3/2}(2)$ | $3d_{5/2}4p_{3/2}(3)$ | $3d_{5/2}4f_{5/2}(4)$ |
| $3p_{1/2}4s_{1/2}(0)$ | $3d_{3/2}4p_{3/2}(1)$ | $3d_{3/2}4p_{1/2}(2)$ | $3d_{3/2}4p_{3/2}(3)$ | $3d_{5/2}4f_{7/2}(4)$ |
| $3p_{3/2}4d_{3/2}(0)$ | $3d_{5/2}4f_{5/2}(1)$ | $3d_{3/2}4p_{3/2}(2)$ | $3d_{5/2}4f_{5/2}(3)$ | $3d_{3/2}4f_{5/2}(4)$ |
| $3s_{1/2}4p_{1/2}(0)$ | $3d_{5/2}4f_{7/2}(1)$ | $3d_{5/2}4f_{5/2}(2)$ | $3d_{5/2}4f_{7/2}(3)$ | $3d_{3/2}4f_{7/2}(4)$ |
| | $3d_{3/2}4f_{5/2}(1)$ | $3d_{5/2}4f_{7/2}(2)$ | $3d_{3/2}4f_{5/2}(3)$ | $3p_{3/2}4d_{5/2}(4)$ |
| | $3p_{3/2}4s_{1/2}(1)$ | $3d_{3/2}4f_{5/2}(2)$ | $3d_{3/2}4f_{7/2}(3)$ | $3s_{1/2}4f_{7/2}(4)$ |
| | $3p_{1/2}4s_{1/2}(1)$ | $3d_{3/2}4f_{7/2}(2)$ | $3p_{3/2}4d_{3/2}(3)$ | $3d_{5/2}4f_{5/2}(5)$ |
| | $3p_{3/2}4d_{3/2}(1)$ | $3p_{3/2}4s_{1/2}(2)$ | $3p_{3/2}4d_{5/2}(3)$ | $3d_{5/2}4f_{7/2}(5)$ |
| | $3p_{3/2}4d_{5/2}(1)$ | $3p_{3/2}4d_{3/2}(2)$ | $3p_{1/2}4d_{5/2}(3)$ | $3d_{3/2}4f_{7/2}(5)$ |
| | $3p_{1/2}4d_{3/2}(1)$ | $3p_{3/2}4d_{5/2}(2)$ | $3s_{1/2}4f_{5/2}(3)$ | $3d_{5/2}4f_{7/2}(6)$ |
| | $3s_{1/2}4p_{1/2}(1)$ | $3p_{1/2}4d_{3/2}(2)$ | $3s_{1/2}4f_{7/2}(3)$ | |
| | $3s_{1/2}4p_{3/2}(1)$ | $3p_{1/2}4d_{5/2}(2)$ | | |
| | | $3s_{1/2}4p_{3/2}(2)$ | | |
| | | $3s_{1/2}4f_{5/2}(2)$ | | |

Even-parity states

| $J=0$ | $J=1$ | $J=2$ | $J=3$ | $J=4$-5 |
|---|---|---|---|---|
| $3d_{5/2}4d_{5/2}(0)$ | $3d_{3/2}4s_{1/2}(1)$ | $3d_{5/2}4s_{1/2}(2)$ | $3d_{5/2}4s_{1/2}(3)$ | $3d_{5/2}4d_{3/2}(4)$ |
| $3d_{3/2}4d_{3/2}(0)$ | $3d_{5/2}4d_{3/2}(1)$ | $3d_{3/2}4s_{1/2}(2)$ | $3d_{5/2}4d_{3/2}(3)$ | $3d_{5/2}4d_{5/2}(4)$ |
| $3p_{3/2}4p_{3/2}(0)$ | $3d_{5/2}4d_{5/2}(1)$ | $3d_{5/2}4d_{3/2}(2)$ | $3d_{5/2}4d_{5/2}(3)$ | $3d_{3/2}4d_{5/2}(4)$ |
| $3p_{1/2}4p_{1/2}(0)$ | $3d_{3/2}4d_{3/2}(1)$ | $3d_{5/2}4d_{5/2}(2)$ | $3d_{3/2}4d_{3/2}(3)$ | $3p_{3/2}4f_{5/2}(4)$ |
| $3s_{1/2}4s_{1/2}(0)$ | $3d_{3/2}4d_{5/2}(1)$ | $3d_{3/2}4d_{3/2}(2)$ | $3d_{3/2}4d_{5/2}(3)$ | $3p_{3/2}4f_{7/2}(4)$ |
| | $3p_{3/2}4p_{1/2}(1)$ | $3d_{3/2}4d_{5/2}(2)$ | $3p_{3/2}4p_{3/2}(3)$ | $3p_{1/2}4f_{7/2}(4)$ |
| | $3p_{3/2}4p_{3/2}(1)$ | $3p_{3/2}4p_{1/2}(2)$ | $3p_{3/2}4f_{5/2}(3)$ | $3d_{5/2}4d_{5/2}(5)$ |
| | $3p_{1/2}4p_{1/2}(1)$ | $3p_{3/2}4p_{3/2}(2)$ | $3p_{1/2}4f_{5/2}(3)$ | $3p_{3/2}4f_{5/2}(5)$ |
| | $3p_{1/2}4p_{3/2}(1)$ | $3p_{1/2}4p_{3/2}(2)$ | $3p_{3/2}4f_{7/2}(3)$ | |
| | $3p_{3/2}4f_{5/2}(1)$ | $3p_{3/2}4f_{5/2}(2)$ | $3p_{1/2}4f_{7/2}(3)$ | |
| | $3s_{1/2}4s_{1/2}(1)$ | $3p_{3/2}4f_{7/2}(2)$ | $3s_{1/2}4d_{5/2}(3)$ | |
| | $3s_{1/2}4d_{3/2}(1)$ | $3p_{1/2}4f_{5/2}(2)$ | | |
| | | $3s_{1/2}4d_{3/2}(2)$ | | |
| | | $3s_{1/2}4d_{5/2}(2)$ | | |

$$E_a^{(2)}=-\sum_{cmn}\sum_k \frac{(-1)^{j_m+j_n-j_a-j_c}}{(2j_a+1)(2k+1)}\frac{X_k(acmn)Z_k(mnac)}{\epsilon_{ac}-\epsilon_{mn}}+\sum_{bcn}\sum_k \frac{(-1)^{j_a+j_n-j_b-j_c}}{(2j_a+1)(2k+1)}\frac{Z_k(bcan)X_k(anbc)}{\epsilon_{bc}-\epsilon_{an}}$$
$$-2\sum_{nb}\delta_{j_bj_n}\sqrt{\frac{2j_b+1}{2j_a+1}}\frac{\Delta(bn)Z_0(naba)}{\epsilon_b-\epsilon_n}, \tag{2.6}$$

where

$$\Delta(bn)=\sum_c \delta_{j_bj_n}\sqrt{\frac{2j_c+1}{2j_b+1}}Z_0(bcnc). \tag{2.7}$$

Labels $b$ and $c$ designate core states, and $m$ and $n$ designate virtual states. The second-order energy for the valence electron $v$ ($E_v^{(2)}$) is found by replacing $a$ by $v$ in the above expression and changing the sign of each term. The second-order particle-hole interaction energies $E^{R_i}([a'v'(J),av(J)]$ are

$$E^{R_1}[a'v'(J),av(J)]=\sum_{mn}\sum_{kk'}(-1)^{J+j_a-j_v}\begin{Bmatrix}k & k' & J\\ j_a & j_v & j_m\end{Bmatrix}\begin{Bmatrix}k & k' & J\\ j_{v'} & j_{a'} & j_n\end{Bmatrix}\frac{X_k(va'mn)Z_{k'}(nmv'a)}{\varepsilon_{va'}-\varepsilon_{nm}}, \tag{2.8}$$

$$E^{R_2}[a'v'(J),av(J)]=\sum_{bc}\sum_{kk'}(-1)^{J+j_a-j_v}\begin{Bmatrix}k & k' & J\\ j_v & j_a & j_b\end{Bmatrix}\begin{Bmatrix}k & k' & J\\ j_{a'} & j_{v'} & j_c\end{Bmatrix}\frac{X_k(bcav')Z_{k'}(a'vcb)}{\varepsilon_{bc}-\varepsilon_{v'a}}, \tag{2.9}$$

$$\begin{aligned}E^{R_3}[a'v'(J),av(J)]=&\frac{1}{(2J+1)^2}\sum_{nb}(-1)^{j_{a'}+j_b-j_{v'}-j_n}\left[\frac{Z_J(a'bv'n)Z_J(vnab)}{\varepsilon_{ba'}-\varepsilon_{v'n}}+\frac{Z_J(vban)Z_J(a'nv'b)}{\varepsilon_{vb}-\varepsilon_{na}}\right]\\&+\sum_{nb}\sum_{k}\frac{1}{2k+1}(-1)^{j_{v'}+j_{a'}+j_b+j_n+k+J}\begin{Bmatrix}j_v & j_a & J\\ j_{a'} & j_{v'} & k\end{Bmatrix}\left[\frac{Z_k(vbv'n)Z_k(a'nab)}{\varepsilon_{bv}-\varepsilon_{v'n}}\right.\\&\left.+\frac{Z_k(a'ban)Z_k(vnv'b)}{\varepsilon_{a'b}-\varepsilon_{na}}\right]\end{aligned} \tag{2.10}$$

$$\begin{aligned}E^{R_4}(a'v'J,avJ)=&\frac{1}{(2J+1)}(-1)^{j_{v'}-j_{a'}+J}\left[\sum_{n\neq v}\delta(j_vj_n)\frac{\Delta(vn)Z_J(na'av')}{\varepsilon_v-\varepsilon_n}+\sum_n\delta(j_{a'}j_n)\frac{\Delta(a'n)Z_J(vnav')}{\varepsilon_{a'}-\varepsilon_n}\right.\\&+\sum_c\delta(j_{v'}j_c)\frac{Z_J(va'ac)\Delta(cv')}{\varepsilon_{v'}-\varepsilon_c}+\sum_{c\neq a}\delta(j_aj_c)\frac{Z_J(va'cv')\Delta(ca)}{\varepsilon_a-\varepsilon_c}+\sum_n\delta(j_aj_n)\frac{Z_J(va'nv')\Delta(na)}{\varepsilon_{va'}-\varepsilon_{nv'}}\\&+\sum_{n(na\neq va')}\delta(j_{v'}j_n)\frac{Z_J(va'an)\Delta(nv')}{\varepsilon_{va'}-\varepsilon_{na}}+\sum_{c(cv\neq v'a)}\delta(j_{a'}j_c)\frac{\Delta(a'c)Z_J(vcav')}{\varepsilon_{v'a}-\varepsilon_{cv}}\\&\left.+\sum_c\delta(j_vj_c)\frac{\Delta(vc)Z_J(ca'av')}{\varepsilon_{v'a}-\varepsilon_{ca'}}\right].\end{aligned} \tag{2.11}$$

All of the above expressions were defined for the Coulomb interaction. When we include the Breit interaction in the calculation, the Coulomb matrix element $X_k(ab,cd)$ is modified according to the rule

$$X_k(ab,cd)\Rightarrow X_k(ab,cd)+M_k(ab,cd)+N_k(ab,cd). \tag{2.12}$$

The magnetic radial integrals $M$ and $N$ are defined by Eqs. (A4) and (A5) in Ref. [19].

### C. Example: Energy matrix for $Ba^{28+}$

In Tables II and III, we give details of the second-order energies for the special case of Ni-like barium, $Z=56$. The headings used in these tables are the same as those used in Ref. [17]. In Table II, we show the second-order contributions to the valence $E_v^{(2)}$ and hole $E_a^{(2)}$ energies, defined in Eq. (2.6). Contributions from each of the three distinct terms—double sum $V_1$, single sum $V_2$, and one-potential term $V_3$—are given in this table. In the upper panels, second-order Coulomb contributions are presented for $n=3$ hole states and $n=4$ particle states and, in the lower panel, second-order Breit-Coulomb corrections are listed. The single sum contribution to hole states dominates the Coulomb corrections shown in the upper panel. The one-potential term $V_3$ contributes only to the Coulomb-Breit correction; where it is the dominant contribution. In Table III we give diagonal matrix elements of the second-order interaction energy for the particle-hole system defined in Eqs. (2.8)–(2.11) for odd-parity states with $J=1$. Coulomb contributions are given in the upper panels, and the Breit-Coulomb corrections are given in the lower ones. The largest contribution is from the term $R_3$ for the Coulomb interaction and from the term $R_4$ for the second-order Breit correction.

The orbitals used in the present calculation were obtained as linear combinations of $B$ splines. These $B$-spline basis orbitals were determined using the method described in Ref. [20]. We used 40 $B$ splines of order 8 for each single-particle angular momentum state, and we included all orbitals with orbital angular momentum $l\leqslant 7$ in our single-particle basis.

In Sec. II B, we gave analytical formulas for the first- and second-order contributions $E^{(1)}[a'v'(J),av(J)]$, $E^{(2)}[a'v'(J),av(J)]$, and $B^{(2)}[a'v'(J),av(J)]$ to the energy matrix. To determine the first-order energies of the states under consideration, we diagonalize the symmetric first-order effective Hamiltonian, including both the Coulomb and Breit interactions. The first-order expansion coefficient $C_1^N[av(J)]$ is the $N$th eigenvector of the first-order effective Hamiltonian, and $E^{(1)}[N]$ is the corresponding eigenvalue. The resulting eigenvectors are used to determine the second-order Coulomb correction $E^{(2)}[N]$, the second-order Breit correction $B^{(2)}[N]$, and the QED correction $E_{\rm Lamb}[N]$. Usually, either $LS$ or $jj$ designations are used to label the resulting eigenvectors rather than simply enunerating with an index $N$. Here we use $jj$ designations, since they are more suitable in Ni-like ions.

In Table IV, we list the following contributions to the energies of odd-parity $J=1$ states in $Ba^{28+}$: $E^{(0+1)}=E^{(0)}$

TABLE II. Contributions to the one-electron $E_v^{(2)}$ and one-hole energy $E_a^{(2)}$ for ions with a $1s^2 2s^2 2p^6 3s^2 3p^6 3d^{10}$ core from the three diagrams $V_1 - V_3$ evaluated for the case of barium, $Z=56$.

(a) Coulomb interaction:

| | $V_1^{\rm HF}$ | $V_2^{\rm HF}$ | $V_3^{\rm HF}$ | $\Sigma^{\rm HF}$ |
|---|---|---|---|---|
| $3s_{1/2}$ | 0.078365 | -0.312162 | | -0.233798 |
| $3p_{1/2}$ | 0.096743 | -0.308099 | | -0.211356 |
| $3p_{3/2}$ | 0.094550 | -0.278281 | | -0.183730 |
| $3d_{3/2}$ | 0.147751 | -0.250838 | | -0.103087 |
| $3d_{5/2}$ | 0.146695 | -0.242938 | | -0.096243 |
| $4s_{1/2}$ | -0.080184 | 0.017005 | | -0.063179 |
| $4p_{1/2}$ | -0.082620 | 0.017788 | | -0.064831 |
| $4p_{3/2}$ | -0.076963 | 0.017584 | | -0.059379 |
| $4d_{3/2}$ | -0.081181 | 0.017376 | | -0.063805 |
| $4d_{5/2}$ | -0.078257 | 0.017296 | | -0.060960 |
| $4f_{5/2}$ | -0.067856 | 0.012001 | | -0.055855 |
| $4f_{7/2}$ | -0.066848 | 0.012194 | | -0.054655 |

(b) Breit correction:

| | $V_1^{\rm BHF}$ | $V_2^{\rm BHF}$ | $V_3^{\rm BHF}$ | $\Sigma^{\rm BHF}$ |
|---|---|---|---|---|
| $3s_{1/2}$ | 0.002252 | -0.001469 | 0.032447 | 0.033230 |
| $3p_{1/2}$ | 0.003539 | -0.001733 | 0.034512 | 0.036319 |
| $3p_{3/2}$ | 0.003093 | -0.001512 | 0.033207 | 0.034788 |
| $3d_{3/2}$ | 0.003933 | -0.002244 | 0.037250 | 0.038939 |
| $3d_{5/2}$ | 0.003370 | -0.001463 | 0.036691 | 0.038598 |
| $4s_{1/2}$ | -0.000596 | 0.000166 | -0.007427 | -0.007856 |
| $4p_{1/2}$ | -0.000817 | 0.000201 | -0.007766 | -0.008381 |
| $4p_{3/2}$ | -0.000738 | 0.000167 | -0.007514 | -0.008084 |
| $4d_{3/2}$ | -0.000820 | 0.000325 | -0.008110 | -0.008605 |
| $4d_{5/2}$ | -0.000822 | 0.000256 | -0.008057 | -0.008623 |
| $4f_{5/2}$ | -0.000607 | 0.000364 | -0.004863 | -0.005107 |
| $4f_{7/2}$ | -0.000508 | 0.000250 | -0.004668 | -0.004926 |

$+E^{(1)}+B^{(1)}$, the second-order Coulomb energy $E^{(2)}$, the second-order Breit correction $B^{(2)}$, the QED correction $E_{\rm Lamb}$, and the total theoretical energy $E^{(\rm tot)}$. The QED correction is approximated as the sum of the one-electron self-energy and the first-order vacuum-polarization energy. The vacuum-polarization contribution is calculated from the Uehling potential using the results of Fullerton and Rinker [21]. The self-energy contribution is estimated for $s$, $p_{1/2}$, and $p_{3/2}$ orbitals by interpolating among the values obtained by Mohr [22] using Coulomb wave functions. For this purpose, an effective nuclear charge $Z_{\rm eff}$ is obtained by finding the value of $Z_{\rm eff}$ required to give a Coulomb orbital with the same average $\langle r \rangle$ as the DHF orbital.

### D. Radiative transitions to the ground state

The first-order reduced multipole matrix element $Z_K^{(1)}$ for a transition between the ground state $|0\rangle$ and the uncoupled particle-hole state $\Phi_{JM}(av)$ of Eq. (2.1) is

$$Z_K^{(1)}[0-av(J)] = \frac{1}{\sqrt{2J+1}} Z_J(av)\,\delta_{JK}. \qquad (2.13)$$

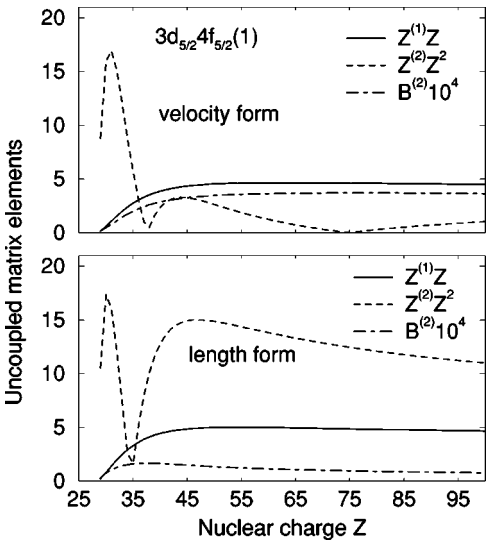


FIG. 1. Uncoupled matrix element for the transition between the $3d_{5/2}4f_{5/2}(1)$ state and the ground state calculated in length and velocity forms in Ni-like ions.

The multipole matrix $Z_K(av)$ element, which includes retardation, can be expressed in terms of the operator $t_K^{(1)}$ given in length and velocity forms by Eqs. (38) and (39), respectively, of Ref. [23] by

$$Z_K(av) = \frac{(2K+1)!!}{k^K} \langle a \| t_K^{(1)} \| v \rangle .$$

The second-order reduced matrix element $Z_K^{(2)}[0-av(J)]$ consists of three contributions: $Z_K^{(\rm RPA)}$, $Z_K^{(\rm HF)}$, and $Z_K^{(\rm derv)}$:

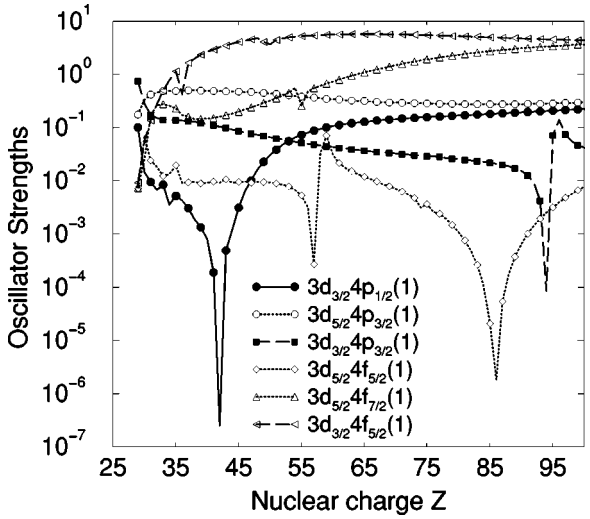


FIG. 2. Oscillator strengths for transitions between the ground state and $3d_j 4p_{j'}(1)$ and $3d_j 4f_{j'}(1)$ states as functions of $Z$.

TABLE III. Diagonal contributions to the second-order interaction term in the effective Hamiltonian matrix from diagrams $R_1$–$R_4$ calculated using HF orbitals. These contributions are given for a hole-particle ion with a $1s^2 2s^2 2p^6 3s^2 3p^6 3d^{10}$ core, and evaluated numerically for the odd-parity states with $J=1$ in the case of barium $Z=56$.

(a) Coulomb interaction:

| | $R_1^{\rm HF}$ | $R_2^{\rm HF}$ | $R_3^{\rm HF}$ | $R_4^{\rm HF}$ | $\Sigma^{\rm HF}$ |
|---|---|---|---|---|---|
| $3d_{3/2}4p_{1/2}$ | 0.004141 | 0.002838 | 0.043857 | | 0.050836 |
| $3d_{5/2}4p_{3/2}$ | 0.004393 | 0.001551 | 0.038373 | | 0.044317 |
| $3d_{3/2}4p_{3/2}$ | 0.006225 | 0.006121 | 0.035867 | | 0.048214 |
| $3d_{5/2}4f_{5/2}$ | 0.005785 | -0.000332 | 0.016577 | | 0.022030 |
| $3d_{5/2}4f_{7/2}$ | 0.005985 | -0.000745 | -0.016659 | | -0.011419 |
| $3d_{3/2}4f_{5/2}$ | 0.005051 | -0.001003 | -0.004367 | | -0.000318 |
| $3p_{3/2}4s_{1/2}$ | 0.002132 | 0.001742 | 0.034175 | | 0.038050 |
| $3p_{1/2}4s_{1/2}$ | 0.002421 | 0.003474 | 0.031964 | | 0.037859 |
| $3p_{3/2}4d_{3/2}$ | 0.003810 | 0.005657 | -0.028107 | | -0.018640 |
| $3p_{3/2}4d_{5/2}$ | 0.003907 | 0.006070 | 0.032414 | | 0.042391 |
| $3p_{1/2}4d_{3/2}$ | 0.002710 | 0.005221 | 0.034010 | | 0.041942 |
| $3s_{1/2}4p_{1/2}$ | 0.002057 | 0.003950 | 0.031657 | | 0.037666 |
| $3s_{1/2}4p_{3/2}$ | 0.001395 | 0.002152 | 0.030924 | | 0.034470 |

(b) Breit corrections:

| | $R_1^{\rm BHF}$ | $R_2^{\rm BHF}$ | $R_3^{\rm BHF}$ | $R_4^{\rm BHF}$ | $\Sigma^{\rm BHF}$ |
|---|---|---|---|---|---|
| $3d_{3/2}4p_{1/2}$ | -0.000029 | -0.000008 | 0.000130 | 0.002129 | 0.002222 |
| $3d_{5/2}4p_{3/2}$ | -0.000018 | -0.000022 | 0.000174 | 0.001556 | 0.001632 |
| $3d_{3/2}4p_{3/2}$ | 0.000012 | -0.000023 | 0.000224 | 0.001654 | 0.001865 |
| $3d_{5/2}4f_{5/2}$ | 0.000003 | 0.000006 | 0.000272 | 0.001054 | 0.001335 |
| $3d_{5/2}4f_{7/2}$ | -0.000058 | -0.000005 | 0.000237 | 0.001019 | 0.001194 |
| $3d_{3/2}4f_{5/2}$ | -0.000027 | -0.000013 | 0.000217 | 0.001248 | 0.001424 |
| $3p_{3/2}4s_{1/2}$ | -0.000003 | -0.000007 | 0.000013 | 0.001364 | 0.001395 |
| $3p_{1/2}4s_{1/2}$ | 0.000017 | 0.000023 | -0.000038 | 0.001553 | 0.001555 |
| $3p_{3/2}4d_{3/2}$ | 0.000001 | -0.000016 | -0.000261 | 0.001561 | 0.001285 |
| $3p_{3/2}4d_{5/2}$ | 0.000006 | -0.000006 | 0.000060 | 0.001172 | 0.001234 |
| $3p_{1/2}4d_{3/2}$ | -0.000007 | -0.000028 | 0.000076 | 0.001566 | 0.001707 |
| $3s_{1/2}4p_{1/2}$ | 0.000015 | 0.000011 | 0.000072 | 0.002074 | 0.002173 |
| $3s_{1/2}4p_{3/2}$ | 0.000001 | 0.000002 | 0.000049 | 0.001410 | 0.001553 |

$$Z_K^{(\rm RPA)}[0-av(J)] = \frac{1}{\sqrt{2J+1}}\delta_{JK}(-1)^{j_b+j_n+K}\frac{1}{2K+1} \times \sum_{b,n}\left[\frac{Z_K(bn)Z_K(anvb)}{\varepsilon_{bv}-\varepsilon_{na}}+\frac{Z_K(abvn)Z_K(nb)}{\varepsilon_{ba}-\varepsilon_{nv}}\right], \tag{2.14}$$

$$Z_K^{(\rm HF)}[0-av(J)] = \frac{1}{\sqrt{2J+1}}\delta_{JK}\sum_n\left[\frac{Z_K(an)\Delta(nv)}{\varepsilon_v-\varepsilon_n}+\frac{\Delta(na)Z_K(nv)}{\varepsilon_a-\varepsilon_n}\right]. \tag{2.15}$$

The derivative term

$$Z_K^{(\rm derv)}(av) = \frac{(2K+1)!!}{k^{K-1}}\langle a\|dt_K^{(1)}/dk\|v\rangle$$

is just the derivative of the first-order matrix element with respect to the transition energy. It is introduced to account for the first-order change in transition energy. An auxillary quantity $P_K^{(\rm derv)}$ is defined by

$$P_K^{(\rm derv)}[0-(av)J] = \frac{1}{\sqrt{2J+1}}Z_J^{(\rm derv)}(av)\delta_{JK}. \tag{2.16}$$

The derivative term $Z_K^{(\rm derv)}(av)$ is given in length and velocity forms by Eqs. (10) and (11) of Ref. [18] for the special case $K=1$.

The coupled dipole transition matrix element between the ground state and the $N$th excited state in Ni-like ions is given by

TABLE IV. Energies of Ni-like barium for odd-parity states with $J=1$ relative to the ground state. $E^{(0+1)} \equiv E^{(0)} + E^{(1)} + B^{(1)}$.

| Level | $E^{(0+1)}$ | $E^{(2)}$ | $B^{(2)}$ | $E_{\mathrm{LAMB}}$ | $E_{\mathrm{tot}}$ |
|---|---|---|---|---|---|
| $3d_{3/2}4p_{1/2}(1)$ | 27.4350 | -0.117082 | 0.032780 | -0.0002 | 27.3505 |
| $3d_{5/2}4p_{3/2}(1)$ | 27.6842 | -0.111305 | 0.032146 | 0.0006 | 27.6056 |
| $3d_{3/2}4p_{3/2}(1)$ | 28.2491 | -0.119704 | 0.032423 | 0.0006 | 28.1624 |
| $3d_{5/2}4f_{5/2}(1)$ | 34.6318 | -0.130068 | 0.034826 | 0.0000 | 34.5366 |
| $3d_{5/2}4f_{7/2}(1)$ | 35.0194 | -0.162317 | 0.034866 | 0.0000 | 34.8919 |
| $3d_{3/2}4f_{5/2}(1)$ | 35.9762 | -0.159260 | 0.035256 | 0.0000 | 35.8522 |
| $3p_{3/2}4s_{1/2}(1)$ | 34.8388 | -0.208859 | 0.028327 | 0.0065 | 34.6648 |
| $3p_{1/2}4s_{1/2}(1)$ | 37.6643 | -0.236676 | 0.030018 | 0.0101 | 37.4677 |
| $3p_{3/2}4d_{3/2}(1)$ | 41.0718 | -0.266175 | 0.027468 | -0.0031 | 40.8300 |
| $3p_{3/2}4d_{5/2}(1)$ | 41.3278 | -0.202299 | 0.027399 | -0.0030 | 41.1499 |
| $3p_{1/2}4d_{3/2}(1)$ | 44.0106 | -0.233219 | 0.029421 | -0.0003 | 43.8065 |
| $3s_{1/2}4p_{1/2}(1)$ | 45.4540 | -0.260963 | 0.027022 | -0.0376 | 45.1825 |
| $3s_{1/2}4p_{3/2}(1)$ | 46.3204 | -0.258707 | 0.026699 | -0.0377 | 46.0507 |

$$Q^{(1+2)}(0-N) = -\frac{1}{E^{(1)}[N]} \sum_{av} C_1^N[av(J)] \times \{[\epsilon_a - \epsilon_v][Z^{(1+2)}[0-av(J)] + B^{(2)}[0-av(J)]] + [-E^{(1)}[N] - \epsilon_a + \epsilon_v]P_1^{(\mathrm{derv})}[0-av(J)]\}. \quad (2.17)$$

Here $Z^{(1+2)} = Z_1^{(1)} + Z_1^{(\mathrm{RPA})}$. (Note that $Z_1^{(\mathrm{HF})}$ vanishes since we start from a HF basis.) In Eq. (2.17), we let $B^{(2)} = B_1^{(\mathrm{RPA})} + B_1^{(\mathrm{HF})}$ represent second-order corrections arising from the Breit interaction. Using the above formulas and the results for uncoupled reduced matrix elements, we transform from uncoupled reduced matrix elements to intermediate coupled matrix elements between physical states.

The uncoupled reduced matrix elements are calculated in both length and velocity gauges. The differences between length and velocity forms are illustrated for the uncoupled $0\text{-}3d_{5/2}4f_{5/2}(1)$ matrix element in Fig. 1. It should be noted that the first-order matrix element $Z^{(1)}$ is proportional $1/Z$, the second-order Coulomb matrix element $Z^{(2)}$ is proportional $1/Z^2$, and the second-order Breit matrix element $B^{(2)}$ is almost independent of $Z$ (see Ref. [18]). Taking into account this dependence, $Z^{(1)} \times Z$, $Z^{(2)} \times Z^2$, and $B^{(2)} \times 10^4$ are shown in the figure. These $Z$ dependencies apply to the first-order matrix elements $Z^{(2)}$, the second-order matrix elements $B^{(2)}$, and the length form of $Z^{(2)}$ for high-$Z$ ions. The contribution of the second-order matrix elements $Z^{(2)}$ is much larger in length form (compare the upper and lower panels in Fig. 1). The differences between results in length and velocity forms shown in Fig. 1 are compensated for by ''derivative terms'' $P^{(\mathrm{derv})}$, as shown below. It should be noted that $P^{(\mathrm{derv})}$ in the length form almost equals $Z^{(1)}$ in length form, whereas $P^{(\mathrm{derv})}$ in velocity form is smaller than $Z^{(1)}$ in velocity form by 3–4 orders of magnitude.

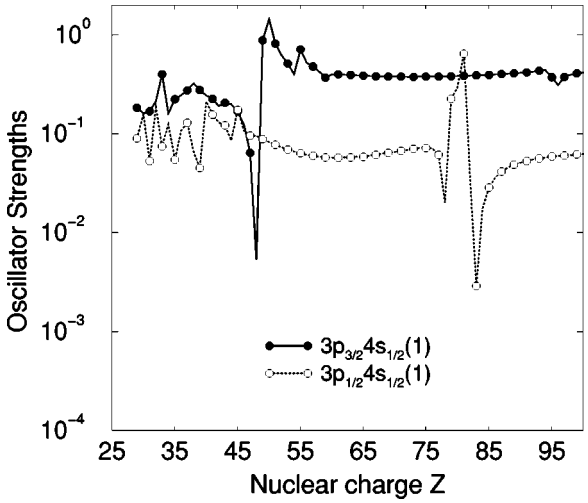


FIG. 3. Oscillator strengths for transitions between the ground state and the $3p_j4s_{1/2}(1)$ state as functions of $Z$.

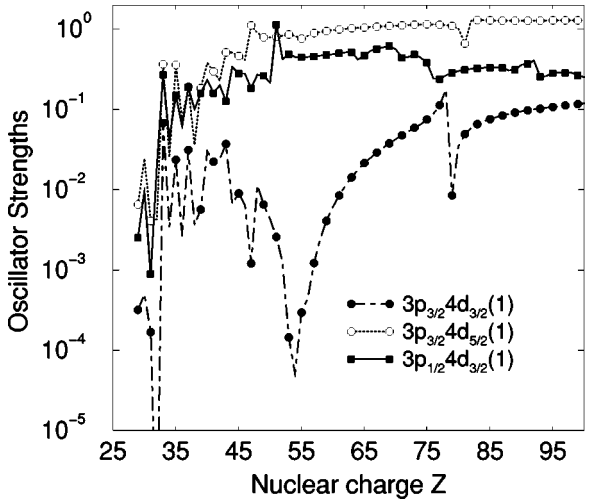


FIG. 4. Oscillator strengths for transitions between the ground state and the $3p_j4d_{j'}(1)$ state as functions of $Z$.

TABLE V. Uncoupled reduced matrix elements in length $L$ and velocity $V$ forms for odd-parity transitions into the ground state in $Ba^{28+}$.

| $av(J)$ | $Z_L^{(1)}$ | $Z_V^{(1)}$ | $Z_L^{(2)}$ | $Z_V^{(2)}$ | $B_L^{(2)}$ | $B_V^{(2)}$ | $P_L^{(\mathrm{derv})}$ | $P_V^{(\mathrm{derv})}$ |
|---|---|---|---|---|---|---|---|---|
| $3d_{3/2}4p_{1/2}(1)$ | 0.087181 | 0.079272 | 0.005138 | 0.005673 | -0.000038 | 0.000008 | 0.086926 | -0.000095 |
| $3d_{5/2}4p_{3/2}(1)$ | -0.105881 | -0.096128 | -0.007742 | -0.007772 | 0.000020 | 0.000082 | -0.105616 | -0.000034 |
| $3d_{3/2}4p_{3/2}(1)$ | 0.033251 | 0.030293 | 0.002660 | 0.002629 | 0.000039 | 0.000083 | 0.033096 | -0.000125 |
| $3d_{5/2}4f_{5/2}(1)$ | -0.089282 | -0.082514 | 0.005098 | 0.001230 | -0.000167 | -0.000413 | -0.089265 | -0.000262 |
| $3d_{5/2}4f_{7/2}(1)$ | 0.398233 | 0.368124 | -0.022676 | -0.005350 | 0.000595 | 0.000771 | 0.396790 | -0.001555 |
| $3d_{3/2}4f_{5/2}(1)$ | -0.327081 | -0.302570 | 0.019714 | 0.005423 | -0.000652 | -0.000891 | -0.326200 | 0.000650 |
| $3p_{3/2}4s_{1/2}(1)$ | 0.104004 | 0.095354 | 0.006651 | 0.007440 | 0.000296 | 0.000261 | 0.103625 | -0.000037 |
| $3p_{1/2}4s_{1/2}(1)$ | 0.059547 | 0.054720 | 0.006430 | 0.006460 | 0.000338 | 0.000346 | 0.059176 | -0.000231 |
| $3p_{3/2}4d_{3/2}(1)$ | 0.061075 | 0.056603 | -0.047905 | -0.042744 | 0.000015 | 0.000116 | 0.060873 | 0.000052 |
| $3p_{3/2}4d_{5/2}(1)$ | 0.176578 | 0.163864 | 0.009530 | 0.011907 | 0.000725 | 0.000955 | 0.175458 | -0.000874 |
| $3p_{1/2}4d_{3/2}(1)$ | -0.115357 | -0.107008 | -0.004076 | -0.005727 | -0.003080 | -0.002986 | -0.114678 | 0.000345 |
| $3s_{1/2}4p_{1/2}(1)$ | 0.070764 | 0.065459 | -0.003999 | -0.002890 | -0.000492 | -0.000343 | 0.070340 | -0.000099 |
| $3s_{1/2}4p_{3/2}(1)$ | -0.082047 | -0.075991 | 0.000546 | 0.000096 | 0.000138 | -0.000083 | -0.081292 | 0.000477 |

### E. Example: Dipole matrix elements in $Ba^{28+}$

In Table V, we list values of *uncoupled* first- and second-order dipole matrix elements $Z^{(1)}$, $Z^{(2)}$, and $B^{(2)}$, together with derivative terms $P^{(\mathrm{derv})}$ for Ni-like barium, $Z=56$. For simplicity, we only list values for the 13 dipole transitions between odd-parity states with $J=1$ and the ground state. The derivative terms shown in Table II arise because transition amplitudes depend on energy, and the transition energy changes order-by-order in MBPT calculations. Both length ($L$) and velocity ($V$) forms are given for the matrix elements. We can see that the first-order matrix elements $Z_L^{(1)}$ and $Z_V^{(1)}$ differ by 10–20 %; the $L$-$V$ differences between second-order matrix elements are much larger for some transitions as seen by comparing $Z_L^{(2)}$ and $Z_V^{(2)}$. It can also seen from Table V that $P^{(\mathrm{derv})}$ in length form almost equals $Z^{(1)}$ in length form but that $P^{(\mathrm{derv})}$ in velocity form is smaller than $Z^{(1)}$ in velocity form by 3–4 orders of magnitude.

Values of *coupled* reduced matrix elements in length and velocity forms are given in Table VI for the transitions considered in Table V. Although we use an intermediate-coupling scheme, it is nevertheless convenient to label the physical states using the $jj$ scheme. We see that $L$ and $V$ forms of the coupled matrix elements in Table VI differ only in the fourth or fifth digits. These $L$-$V$ differences arise because we start our MBPT calculations using a non-local Dirac-Fock (DF) potential. If we were to replace the DF potential by a local potential, the differences would disappear completely. The last two columns in Table VI show $L$ and $V$ values of *coupled* reduced matrix elements calculated without the second-order contribution. As can be seen from this table, removing the second-order contribution increases the $L$-$V$ differences.

It should be emphasized that we include negative-energy-state (NES) contributions to sums over intermediate states. Ignoring the NES contributions leads to small changes in the $L$-form matrix elements, but substantial changes in some of the $V$-form matrix elements, with a consequent loss of gauge independence.

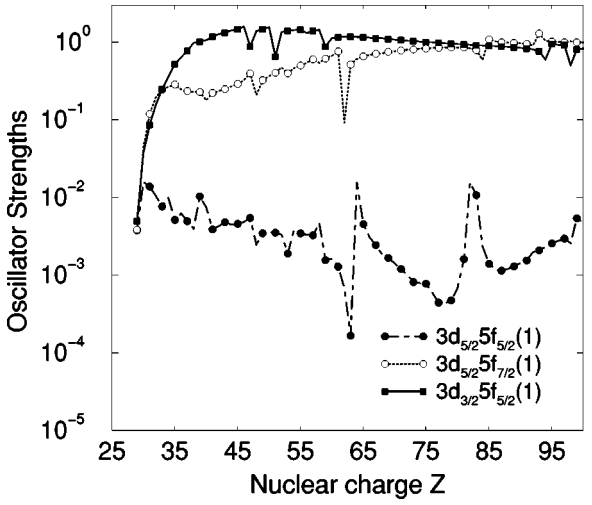


FIG. 5. Oscillator strengths for transitions between the ground state and the $3d_j5f_{j'}(1)$ state as functions of $Z$.

TABLE VI. Coupled reduced matrix elements in length $L$ and velocity $V$ forms for odd-parity transitions into the ground state in $Ba^{28+}$.

| | MBPT | | First order | |
|---|---|---|---|---|
| $av(J)$ | $L$ | $V$ | $L$ | $V$ |
| $3d_{3/2}4p_{1/2}(1)$ | -0.068287 | -0.067912 | -0.064126 | -0.058401 |
| $3d_{5/2}4p_{3/2}(1)$ | -0.140705 | -0.140013 | -0.132503 | -0.120496 |
| $3d_{3/2}4p_{3/2}(1)$ | 0.050965 | 0.050680 | 0.047335 | 0.043148 |
| $3d_{5/2}4f_{5/2}(1)$ | -0.011981 | -0.011825 | -0.011005 | -0.010230 |
| $3d_{5/2}4f_{7/2}(1)$ | -0.145601 | -0.145668 | -0.154598 | -0.142856 |
| $3d_{3/2}4f_{5/2}(1)$ | 0.467167 | 0.467484 | 0.496550 | 0.459288 |
| $3p_{3/2}4s_{1/2}(1)$ | 0.148537 | 0.148052 | 0.144775 | 0.133128 |
| $3p_{1/2}4s_{1/2}(1)$ | -0.051011 | -0.050367 | -0.041079 | -0.037665 |
| $3p_{3/2}4d_{3/2}(1)$ | 0.046451 | 0.042222 | -0.003995 | -0.003625 |
| $3p_{3/2}4d_{5/2}(1)$ | 0.170504 | 0.170879 | 0.176448 | 0.163761 |
| $3p_{1/2}4d_{3/2}(1)$ | 0.124708 | 0.123974 | 0.115723 | 0.107345 |
| $3s_{1/2}4p_{1/2}(1)$ | -0.040535 | -0.040678 | -0.043162 | -0.039890 |
| $3s_{1/2}4p_{3/2}(1)$ | -0.062830 | -0.063085 | -0.065063 | -0.060257 |

TABLE VII. Wavelengths (λ in Å) for Ni-like ions for odd-parity states with $J=1$ given relative to the ground state. Comparison with experimental results presented in Refs. [10], [11], and [14].

| | $3d_{3/2}4p_{1/2}$ | $3d_{5/2}4p_{3/2}$ | $3d_{3/2}4p_{3/2}$ | $3d_{5/2}4f_{5/2}$ | $3d_{5/2}4f_{7/2}$ | $3d_{3/2}4f_{5/2}$ | $3p_{3/2}4s_{1/2}$ | $3p_{1/2}4s_{1/2}$ | $3p_{3/2}4d_{3/2}$ | $3p_{3/2}4d_{5/2}$ | $3p_{1/2}4d_{3/2}$ |
|---|---|---|---|---|---|---|---|---|---|---|---|
| $Z=47$ | 31.491 | 31.242 | 30.812 | 23.601 | 23.397 | 22.852 | 22.561 | 21.329 | 18.814 | 18.706 | 17.888 |
| $\lambda_{expt}$ [14] | 31.427 | 31.189 | 30.757 | 23.571 | 23.333 | 22.821 | | | | | |
| $Z=48$ | 28.986 | 28.760 | 28.345 | 21.897 | 21.704 | 21.187 | 21.069 | 19.914 | 17.612 | 17.512 | 16.713 |
| $\lambda_{expt}$ [14] | 28.934 | 28.716 | 28.301 | 21.970 | 21.450 | 21.160 | | | | | |
| $Z=49$ | 26.777 | 26.570 | 26.169 | 20.379 | 20.196 | 19.727 | 19.702 | 18.593 | 16.516 | 16.428 | 15.657 |
| $\lambda_{expt}$ [14] | 26.735 | 26.533 | 26.131 | | 20.040 | 19.710 | | | | | |
| $Z=50$ | 24.820 | 24.627 | 24.238 | 19.020 | 18.846 | 18.359 | 18.527 | 17.402 | 15.541 | 15.450 | 14.692 |
| $\lambda_{expt}$ [14] | 24.785 | 24.596 | 24.211 | 19.027 | 18.811 | 18.356 | | | | | |
| $Z=51$ | 23.076 | 22.894 | 22.522 | 17.798 | 17.633 | 17.176 | 17.414 | 16.321 | 14.640 | 14.554 | 13.814 |
| $Z=52$ | 21.516 | 21.342 | 20.981 | 16.694 | 16.537 | 16.106 | 16.403 | 15.337 | 13.818 | 13.736 | 13.011 |
| $Z=53$ | 20.113 | 19.946 | 19.595 | 15.694 | 15.543 | 15.135 | 15.480 | 14.438 | 13.064 | 12.985 | 12.275 |
| $Z=54$ | 18.847 | 18.686 | 18.339 | 14.784 | 14.639 | 14.252 | 14.634 | 13.614 | 12.371 | 12.295 | 11.600 |
| $\lambda_{expt}$ [14] | 18.826 | 18.667 | 18.326 | | 14.618 | | | | | | |
| $Z=55$ | 17.701 | 17.544 | 17.210 | 13.953 | 13.813 | 13.446 | 13.859 | 12.857 | 11.727 | 11.659 | 10.977 |
| $Z=56$ | 16.659 | 16.505 | 16.179 | 13.193 | 13.058 | 12.709 | 13.144 | 12.161 | 11.159 | 11.072 | 10.401 |
| $\lambda_{expt}$ [10] | | | | | 13.046 | 12.721 | 13.136 | | 11.072 | 10.388 | |
| $Z=57$ | 15.709 | 15.558 | 15.239 | 12.495 | 12.365 | 12.032 | 12.484 | 11.518 | 10.600 | 10.503 | 9.868 |
| $\lambda_{expt}$ [11] | | | | | 12.335 | 12.020 | 12.458 | | 10.512 | 9.841 | |
| $Z=58$ | 14.841 | 14.692 | 14.379 | 11.856 | 11.727 | 11.409 | 11.870 | 10.923 | 10.093 | 10.027 | 9.374 |
| $Z=59$ | 14.045 | 13.897 | 13.591 | 11.257 | 11.138 | 10.834 | 11.310 | 10.372 | 9.622 | 9.557 | 8.915 |
| $\lambda_{expt}$ [11] | | | | 11.256 | 11.129 | 10.842 | 11.310 | | | 9.559 | 8.915 |
| $Z=60$ | 13.313 | 13.167 | 12.866 | 10.709 | 10.594 | 10.303 | 10.785 | 9.861 | 9.184 | 9.121 | 8.487 |
| $Z=61$ | 12.639 | 12.493 | 12.199 | 10.201 | 10.089 | 9.810 | 10.296 | 9.385 | 8.775 | 8.713 | 8.088 |
| $Z=62$ | 12.016 | 11.871 | 11.580 | 9.729 | 9.620 | 9.352 | 9.841 | 8.941 | 8.393 | 8.333 | 7.716 |
| $\lambda_{expt}$ [14] | 11.950 | 11.830 | 11.530 | 9.785 | 9.620 | | 9.850 | | | | |
| $Z=63$ | 11.440 | 11.295 | 11.011 | 9.289 | 9.184 | 8.926 | 9.417 | 8.527 | 8.036 | 7.976 | 7.367 |
| $Z=64$ | 10.905 | 10.761 | 10.479 | 8.880 | 8.777 | 8.529 | 9.020 | 8.140 | 7.701 | 7.642 | 7.040 |
| $\lambda_{expt}$ [14] | 10.900 | 10.750 | 10.470 | | 8.770 | 8.530 | 9.010 | | | 7.638 | |
| $Z=65$ | 10.409 | 10.265 | 9.989 | 8.497 | 8.398 | 8.158 | 8.648 | 7.778 | 7.387 | 7.329 | 6.734 |
| $Z=66$ | 9.947 | 9.803 | 9.529 | 8.139 | 8.043 | 7.811 | 8.299 | 7.438 | 7.091 | 7.034 | 6.446 |
| $\lambda_{expt}$ [14] | 9.960 | 9.810 | 9.540 | | 8.020 | 7.820 | 8.280 | | | | |
| $Z=67$ | 9.516 | 9.372 | 9.103 | 7.804 | 7.710 | 7.486 | 7.972 | 7.119 | 6.813 | 6.757 | 6.175 |
| $Z=68$ | 9.113 | 8.969 | 8.704 | 7.489 | 7.398 | 7.181 | 7.665 | 6.819 | 6.551 | 6.495 | 5.920 |
| $Z=69$ | 8.737 | 8.592 | 8.329 | 7.193 | 7.104 | 6.894 | 7.375 | 6.537 | 6.304 | 6.249 | 5.678 |
| $\lambda_{expt}$ [14] | 8.734 | 8.591 | 8.326 | 7.184 | 7.099 | 6.890 | 7.370 | 6.528 | 6.296 | 6.245 | 5.655 |
| $Z=70$ | 8.384 | 8.239 | 7.979 | 6.915 | 6.829 | 6.624 | 7.103 | 6.270 | 6.071 | 6.016 | 5.459 |
| $\lambda_{expt}$ [14] | 8.377 | 8.235 | 7.978 | 6.914 | 6.822 | 6.620 | 7.099 | 6.270 | 6.061 | 6.01 | 5.44 |
| $Z=71$ | 8.053 | 7.908 | 7.652 | 6.653 | 6.569 | 6.369 | 6.845 | 6.019 | 5.850 | 5.795 | 5.205 |
| $Z=72$ | 7.743 | 7.596 | 7.342 | 6.406 | 6.323 | 6.129 | 6.603 | 5.782 | 5.641 | 5.587 | 5.006 |
| $\lambda_{expt}$ [14] | 7.739 | 7.594 | 7.339 | 6.419 | 6.317 | 6.125 | 6.596 | 5.780 | 5.640 | 5.586 | |
| $Z=73$ | 7.450 | 7.303 | 7.052 | 6.172 | 6.092 | 5.902 | 6.373 | 5.558 | 5.443 | 5.389 | 4.816 |
| $\lambda_{expt}$ [14] | 7.447 | 7.301 | 7.051 | 6.176 | 6.092 | 5.907 | 6.370 | | 5.43 | 5.382 | 4.818 |
| $Z=74$ | 7.175 | 7.027 | 6.779 | 5.951 | 5.873 | 5.687 | 6.156 | 5.345 | 5.255 | 5.202 | 4.635 |
| $\lambda_{expt}$ [14] | 7.172 | 7.024 | 6.775 | 5.956 | 5.871 | 5.689 | 6.154 | | 5.247 | 5.200 | 4.638 |
| $Z=75$ | 6.916 | 6.767 | 6.521 | 5.742 | 5.666 | 5.484 | 5.950 | 5.144 | 5.077 | 5.024 | 4.463 |
| $\lambda_{expt}$ [14] | 6.914 | 6.765 | 6.518 | 5.740 | 5.663 | 5.484 | 5.943 | | | 5.025 | 4.464 |
| $Z=76$ | 6.671 | 6.521 | 6.278 | 5.544 | 5.470 | 5.292 | 5.755 | 4.953 | 4.907 | 4.854 | 4.298 |
| $Z=77$ | 6.440 | 6.289 | 6.048 | 5.356 | 5.284 | 5.109 | 5.570 | 4.773 | 4.745 | 4.693 | 4.142 |
| $Z=78$ | 6.221 | 6.069 | 5.829 | 5.178 | 5.107 | 4.936 | 5.394 | 4.588 | 4.604 | 4.540 | 3.992 |
| $\lambda_{expt}$ [14] | 6.214 | 6.062 | 5.824 | 5.179 | 5.098 | 4.932 | | | | 4.539 | 3.993 |

TABLE VII. (*Continued*).

| | $3d_{3/2}4p_{1/2}$ | $3d_{5/2}4p_{3/2}$ | $3d_{3/2}4p_{3/2}$ | $3d_{5/2}4f_{5/2}$ | $3d_{5/2}4f_{7/2}$ | $3d_{3/2}4f_{5/2}$ | $3p_{3/2}4s_{1/2}$ | $3p_{1/2}4s_{1/2}$ | $3p_{3/2}4d_{3/2}$ | $3p_{3/2}4d_{5/2}$ | $3p_{1/2}4d_{3/2}$ |
|---|---|---|---|---|---|---|---|---|---|---|---|
| $Z=79$ | 6.014 | 5.860 | 5.623 | 5.009 | 4.939 | 4.771 | 5.227 | 4.430 | 4.452 | 4.394 | 3.850 |
| $\lambda_{expt}$ [14] | 6.010 | 5.850 | 5.620 | | 4.930 | 4.760 | 5.222 | | | | 3.851 |
| $Z=80$ | 5.818 | 5.663 | 5.427 | 4.847 | 4.780 | 4.614 | 5.068 | 4.277 | 4.309 | 4.254 | 3.714 |
| $\lambda_{expt}$ [14] | 5.816 | 5.657 | 5.417 | | 4.771 | 4.609 | 5.055 | | | 4.252 | 3.714 |
| $Z=81$ | 5.632 | 5.475 | 5.243 | 4.694 | 4.628 | 4.464 | 4.916 | 4.131 | 4.176 | 4.119 | 3.584 |
| $Z=82$ | 5.455 | 5.297 | 5.065 | 4.548 | 4.483 | 4.322 | 4.772 | 3.984 | 4.049 | 3.998 | 3.461 |
| $\lambda_{expt}$ [14] | 5.454 | 5.291 | 5.055 | | 4.475 | 4.318 | 4.759 | | | 3.998 | |
| $Z=83$ | 5.287 | 5.128 | 4.898 | 4.409 | 4.345 | 4.186 | 4.635 | 3.849 | 3.927 | 3.875 | 3.342 |
| $Z=84$ | 5.128 | 4.967 | 4.739 | 4.276 | 4.214 | 4.056 | 4.504 | 3.720 | 3.811 | 3.759 | 3.230 |
| $Z=85$ | 4.976 | 4.813 | 4.587 | 4.149 | 4.088 | 3.933 | 4.379 | 3.597 | 3.700 | 3.648 | 3.119 |
| $Z=86$ | 4.832 | 4.667 | 4.442 | 4.027 | 3.968 | 3.814 | 4.260 | 3.479 | 3.594 | 3.542 | 3.015 |
| $Z=87$ | 4.694 | 4.527 | 4.304 | 3.911 | 3.853 | 3.701 | 4.145 | 3.365 | 3.492 | 3.440 | 2.916 |
| $Z=88$ | 4.563 | 4.394 | 4.172 | 3.800 | 3.743 | 3.593 | 4.036 | 3.257 | 3.394 | 3.342 | 2.820 |
| $Z=89$ | 4.438 | 4.266 | 4.046 | 3.694 | 3.638 | 3.489 | 3.932 | 3.153 | 3.300 | 3.249 | 2.728 |
| $Z=90$ | 4.319 | 4.145 | 3.925 | 3.592 | 3.537 | 3.389 | 3.832 | 3.053 | 3.210 | 3.159 | 2.640 |
| $Z=91$ | 4.205 | 4.028 | 3.810 | 3.494 | 3.441 | 3.294 | 3.737 | 2.957 | 3.124 | 3.073 | 2.555 |
| $Z=92$ | 4.096 | 3.917 | 3.700 | 3.401 | 3.348 | 3.202 | 3.645 | 2.865 | 3.041 | 2.990 | 2.474 |

## III. X-RAY WAVELENGTHS FOR NI-LIKE IONS $Z=47-92$

The $n=3-4$ transitions in Ni-like ions have been thoroughly investigated, theoretically and experimentally. In Table VII, our MBPT results of wavelengths for transitions from 11 excited $J=1$ states to the ground state are compared with experimental data given in Refs. [10], [11], and [14]. Other references to experimental measurements were omitted since they were included by Quinet and Biémont in Ref. [14]. The $n=3-4$ transitions observed in x-ray spectra of the Ni-like ions $Ag^{19+}$-$Pb^{54+}$ were investigated theoretically in Ref. [14] using the multiconfigurational Dirac-Fock approach. Our MBPT method starts from the Dirac-Fock approximation, and includes correlation corrections for Coulomb-Coulomb ($E^{(2)}$) and Coulomb-Breit $B^{(2)}$) interactions. The correlation corrections are in the range 2000–10 000 $cm^{-1}$, as seen in Table IV. Consequently, our MBPT data in Table VII are in closer agreement with experimental data than the uncorrelated values from Ref. [14], and can be used to predict wavelengths in future experiments.

TABLE VIII. Wavelengths ($\lambda$ in Å) for $3d4p(J)$-$3d4d(J')$ transitions in Ni-like ions. Comparison with experimental data ($\lambda_{expt}$) and predicted data ($\lambda_{fit}$) from Scofield and MacGowan in Ref. [5].

| | $3d_{5/2}4p_{3/2}(1)$-$3d_{5/2}4d_{5/2}(2)$ | | | $3d_{5/2}4p_{3/2}(1)$-$3d_{5/2}4d_{5/2}(1)$ | | |
|---|---|---|---|---|---|---|
| $Z$ | $\lambda_{MBPT}$ | $\lambda_{fit}$ | $\lambda_{expt}$ | $\lambda_{MBPT}$ | $\lambda_{fit}$ | $\lambda_{expt}$ |
| 47 | 188.49 | 189.06 | | 195.54 | 195.83 | |
| 48 | 179.26 | 179.73 | | 186.05 | 186.26 | |
| 49 | 170.84 | 171.23 | | 177.39 | 177.56 | |
| 50 | 163.15 | 163.49 | | 169.47 | 169.58 | |
| 54 | 137.85 | 138.04 | | 143.39 | 143.47 | |
| 62 | 103.68 | 103.72 | | 108.01 | 108.01 | |
| 64 | 97.24 | 97.26 | | 101.31 | 101.30 | |
| 66 | 91.38 | 91.38 | | 95.21 | 95.19 | |
| 69 | 83.51 | 83.50 | | 87.00 | 86.97 | |
| 70 | 81.39 | 81.08 | 81.07 | 84.48 | 84.45 | 84.41 |
| 72 | 76.81 | 76.53 | | 79.73 | 79.69 | |
| 73 | 74.63 | 74.38 | 74.42 | 77.48 | 77.45 | 77.47 |
| 74 | 72.54 | 72.31 | 72.40 | 75.32 | 75.28 | 75.35 |
| 75 | 70.49 | 70.32 | | 73.23 | 73.19 | |
| 78 | 64.83 | 64.73 | | 67.38 | 67.34 | |
| 79 | 63.08 | 62.99 | | 65.56 | 65.51 | |
| 80 | 61.39 | 61.30 | | 63.79 | 63.74 | |
| 82 | 58.18 | 58.09 | | 60.43 | 60.38 | |

## IV. WAVELENGTHS OF TRANSITIONS BETWEEN EXCITED STATES

Transitions between excited states were studied mostly for purpose of obtaining accurate data for lasing

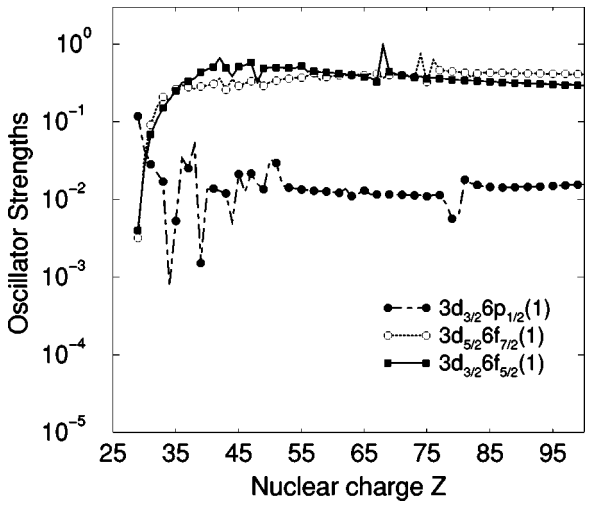


FIG. 6. Oscillator strengths for transitions between the ground state and the $3d_j6f_{j'}(1)$ state as functions of $Z$.

TABLE IX. Wavelengths (λ in Å) for $3d4s(J)$-$3d4p(J')$ transitions in Ni-like ions. Comparison with experimental results from Churilov *et al.* in Ref. [15].

| $3dj4s(J)$ | $3dj4pj'(J')$ | $Z=47$ | | $Z=48$ | | $Z=49$ | | $Z=50$ | |
|---|---|---|---|---|---|---|---|---|---|
| | | $\lambda_{MBPT}$ | $\lambda_{expt}$ | $\lambda_{MBPT}$ | $\lambda_{expt}$ | $\lambda_{MBPT}$ | $\lambda_{expt}$ | $\lambda_{MBPT}$ | $\lambda_{expt}$ |
| $3d_{5/2}4s(3)$ | $3d_{3/2}4p_{3/2}(2)$ | 221.856 | | 207.389 | | 194.109 | | 181.878 | |
| $3d_{5/2}4s(2)$ | $3d_{3/2}4p_{3/2}(2)$ | 225.089 | | 210.357 | | 196.817 | | 184.358 | |
| $3d_{5/2}4s(3)$ | $3d_{3/2}4p_{3/2}(3)$ | 227.142 | | 212.179 | | 198.446 | | 185.809 | |
| $3d_{5/2}4s(2)$ | $3d_{3/2}4p_{3/2}(1)$ | 229.072 | | 214.124 | | 200.348 | | 187.676 | |
| $3d_{5/2}4s(2)$ | $3d_{3/2}4p_{3/2}(3)$ | 230.532 | | 215.287 | | 201.277 | | 188.398 | |
| $3d_{5/2}4s(3)$ | $3d_{5/2}4p_{3/2}(3)$ | 248.581 | 248.745 | 233.874 | 234.043 | 220.335 | 220.593 | 207.828 | 207.988 |
| $3d_{3/2}4s(1)$ | $3d_{3/2}4p_{3/2}(2)$ | 250.082 | 250.292 | 235.299 | 235.536 | 221.697 | 221.977 | 209.115 | 209.288 |
| $3d_{5/2}4s(2)$ | $3d_{5/2}4p_{3/2}(3)$ | 252.647 | 252.820 | 237.656 | 237.859 | 223.831 | 224.106 | 211.072 | |
| $3d_{3/2}4s(2)$ | $3d_{3/2}4p_{3/2}(2)$ | 253.505 | 253.685 | 238.402 | 238.614 | 224.515 | 224.745 | 211.689 | 211.845 |
| $3d_{5/2}4s(3)$ | $3d_{5/2}4p_{3/2}(2)$ | 253.505 | | 238.601 | | 224.859 | | 212.143 | |
| $3d_{3/2}4s(1)$ | $3d_{3/2}4p_{3/2}(1)$ | 255.008 | 254.992 | 240.022 | 240.074 | 226.187 | 226.242 | 213.395 | |
| $3d_{5/2}4s(2)$ | $3d_{5/2}4p_{3/2}(1)$ | 255.165 | 240.258 | 240.288 | 226.430 | 226.524 | 213.631 | 213.765 | |
| $3d_{5/2}4s(2)$ | $3d_{5/2}4p_{3/2}(2)$ | 257.735 | 258.045 | 242.539 | 242.817 | 228.501 | 228.802 | 215.525 | 215.745 |
| $3d_{3/2}4s(2)$ | $3d_{3/2}4p_{3/2}(1)$ | 258.568 | | 243.251 | | 229.122 | | 216.077 | |
| $3d_{3/2}4s(2)$ | $3d_{3/2}4p_{3/2}(3)$ | 260.430 | 260.485 | 244.754 | 244.850 | 230.338 | 230.478 | 217.034 | 217.135 |
| $3d_{5/2}4s(3)$ | $3d_{5/2}4p_{3/2}(4)$ | 260.759 | 260.875 | 245.096 | 245.222 | 230.687 | 230.895 | 217.386 | 217.493 |
| $3d_{3/2}4s(1)$ | $3d_{3/2}4p_{3/2}(0)$ | 270.031 | 270.010 | 253.609 | 253.677 | 238.513 | 238.777 | 224.575 | |
| $3d_{5/2}4s(3)$ | $3d_{3/2}4p_{1/2}(2)$ | 272.258 | 272.133 | 256.999 | | 242.951 | | 229.995 | |
| $3d_{5/2}4s(2)$ | $3d_{3/2}4p_{1/2}(1)$ | 272.795 | 272.133 | 257.028 | 256.410 | 242.577 | | 229.299 | |
| $3d_{5/2}4s(2)$ | $3d_{3/2}4p_{1/2}(2)$ | 277.143 | | 261.573 | | 247.209 | | 233.975 | |
| $3d_{3/2}4s(1)$ | $3d_{5/2}4p_{3/2}(1)$ | 287.767 | | 273.391 | | 260.122 | | 247.779 | 247.920 |
| $3d_{3/2}4s(2)$ | $3d_{5/2}4p_{3/2}(3)$ | 289.009 | | 274.081 | | 260.360 | | 247.685 | |
| $3d_{3/2}4s(1)$ | $3d_{5/2}4p_{3/2}(2)$ | 291.039 | 291.713 | 276.309 | | 262.732 | | 250.146 | 250.780 |
| $3d_{3/2}4s(2)$ | $3d_{5/2}4p_{3/2}(1)$ | 292.309 | 292.568 | 277.588 | 277.851 | 264.011 | 264.206 | 251.402 | 251.524 |
| $3d_{3/2}4s(2)$ | $3d_{5/2}4p_{3/2}(2)$ | 295.686 | | 280.597 | | 266.700 | | 253.839 | |
| $3d_{3/2}4s(1)$ | $3d_{3/2}4p_{1/2}(1)$ | 310.390 | | 295.272 | | 281.514 | | 268.895 | |
| $3d_{5/2}4s(3)$ | $3d_{5/2}4p_{1/2}(3)$ | 310.856 | 311.039 | 296.443 | 296.622 | 283.247 | 283.448 | 271.071 | 271.264 |
| $3d_{3/2}4s(2)$ | $3d_{3/2}4p_{1/2}(1)$ | 315.680 | 315.041 | 300.174 | 299.660 | 286.075 | 285.667 | 273.167 | |
| $3d_{3/2}4s(1)$ | $3d_{3/2}4p_{1/2}(2)$ | 316.031 | 315.952 | 301.285 | 301.276 | 287.772 | 287.791 | 275.346 | 275.368 |
| $3d_{5/2}4s(2)$ | $3d_{5/2}4p_{1/2}(3)$ | 317.241 | 317.408 | 302.545 | 302.800 | 289.051 | 289.298 | 276.617 | 276.809 |
| $3d_{5/2}4s(3)$ | $3d_{5/2}4p_{1/2}(2)$ | 318.105 | 317.932 | 303.089 | 302.972 | 289.363 | 289.298 | 276.735 | 276.651 |
| $3d_{3/2}4s(2)$ | $3d_{3/2}4p_{1/2}(2)$ | 321.517 | | 306.390 | 306.315 | 292.540 | | 279.828 | |
| $3d_{5/2}4s(2)$ | $3d_{5/2}4p_{1/2}(2)$ | 324.793 | | 309.471 | 309.390 | 295.423 | | 282.517 | |
| $3d_{3/2}4s(2)$ | $3d_{5/2}4p_{1/2}(3)$ | 376.763 | | 364.157 | | 353.010 | | 343.080 | |
| $3d_{3/2}4s(1)$ | $3d_{5/2}4p_{1/2}(2)$ | 379.524 | | 366.648 | | 355.266 | | 345.133 | |
| $3d_{3/2}4s(2)$ | $3d_{5/2}4p_{1/2}(2)$ | 387.463 | | 374.237 | | 362.561 | | 352.203 | |

lines. In Table VIII, our MBPT wavelengths for the two lasing lines $3d_{5/2}4p_{3/2}(1)$-$3d_{5/2}4d_{5/2}(2)$ and $3d_{5/2}4p_{3/2}(1)$-$3d_{5/2}4d_{5/2}(1)$ are compared with predicted and experimental values given by Scofield and MacGowan in Ref. [5] for ions in the range $Z=47$–82. The prediction in Ref. [5] was obtained by a semiempirical fit to the experimental measurement given in Table VIII.

Our MBPT calculations are in a good agreement with the three experimental values and with predicted data in interval $Z=62$–82 for the $3d_{5/2}4p_{3/2}(1)$-$3d_{5/2}4d_{5/2}(1)$ line. There is also a good agreement with predicted data for the $3d_{5/2}4p_{3/2}(1)$–$3d_{5/2}4d_{5/2}(2)$ line in intervals $Z=62$–69 and 78–82. However our MBPT calculations for this line disagrees with experimental and predicted data in the range of $Z=70$–73. We have no explanation for this disagreement.

In Table IX, our MBPT results of wavelengths for $3d_{j_1}4s_{1/2}(J)$-$3d_{j_2}4p_j(J')$ transitions are compared with experimental data given in Ref. [15]. The identification given in Ref. [15] for $\Delta n=0$ transitions in the spectra of four Ni-like ions with $Z=47$–50 was based on the Slater-Condon method with generalized least-square (GLS) fits of energy parameters. This method was described by Wyart [16]. As can be seen from Table IX, our MBPT data are in a good agreement with experimental data: the disagreement in $3d_{j_1}4s_{1/2}(J)$-$3d_{j_2}4p_j(J')$ wavelengths is about 0.07%, except for three lines [$3d_{5/2}4s_{1/2}(2)$-$3d_{3/2}4p_{1/2}(1)$ in $Cd^{20+}$, $3d_{3/2}4s_{1/2}(2)$-$3d_{3/2}4p_{1/2}(1)$ in $In^{21+}$, and

TABLE X. Wavelengths ($\lambda$ in Å) for $3d4p(J)$-$3d4d(J')$ transitions in Ni-like ions. Comparison with experimental data ($\lambda_{expt}$) from Churilov *et al.* in Ref. [15] and predicted data ($\lambda_{GLS}$) from Wyart in Ref. [16].

| $3dj4pj'(J)$ | $3dj4pj'(J')$ | $Z=47$ | | $Z=48$ | | $Z=49$ | | $Z=50$ | |
|---|---|---|---|---|---|---|---|---|---|
| | | $\lambda_{MBPT}$ | $\lambda_{GLS}$ | $\lambda_{MBPT}$ | $\lambda_{GLS}$ | $\lambda_{MBPT}$ | $\lambda_{GLS}$ | $\lambda_{MBPT}$ | $\lambda_{GLS}$ |
| $3d_{5/2}4p_{1/2}(3)$ | $3d_{5/2}4d_{5/2}(4)$ | 164.228 | | 154.962 | | 146.459 | | 138.630 | |
| $3d_{3/2}4p_{1/2}(2)$ | $3d_{3/2}4d_{5/2}(2)$ | 164.631 | | 155.406 | | 146.931 | | 139.112 | |
| $3d_{5/2}4p_{1/2}(3)$ | $3d_{5/2}4d_{5/2}(2)$ | 164.685 | | 155.400 | | 146.879 | | 139.036 | |
| $3d_{3/2}4p_{1/2}(2)$ | $3d_{3/2}4d_{3/2}(2)$ | 165.318 | 165.336 | 156.323 | 156.303 | 148.082 | 148.010 | 140.480 | 140.360 |
| $3d_{5/2}4p_{1/2}(3)$ | $3d_{5/2}4d_{5/2}(3)$ | 165.878 | 165.635 | 156.521 | 156.217 | 147.938 | 147.567 | 140.031 | 139.588 |
| $3d_{5/2}4p_{1/2}(2)$ | $3d_{5/2}4d_{3/2}(3)$ | 166.752 | 166.845 | 157.675 | 157.717 | 149.354 | 149.333 | 141.677 | 141.600 |
| $3d_{3/2}4p_{1/2}(1)$ | $3d_{3/2}4d_{3/2}(2)$ | 166.905 | | 157.992 | | 149.796 | | 142.221 | |
| $3d_{5/2}4p_{1/2}(2)$ | $3d_{5/2}4d_{5/2}(1)$ | 167.951 | | 158.597 | | 149.998 | | 142.061 | |
| $3d_{3/2}4p_{1/2}(2)$ | $3d_{3/2}4d_{5/2}(1)$ | 168.304 | | 158.907 | | 150.280 | | 142.305 | |
| $3d_{5/2}4p_{1/2}(3)$ | $3d_{5/2}4d_{3/2}(3)$ | 168.816 | 168.796 | 159.536 | 159.481 | 151.037 | 150.933 | 143.209 | 143.056 |
| $3d_{5/2}4p_{1/2}(2)$ | $3d_{5/2}4d_{3/2}(2)$ | 168.991 | 168.862 | 159.782 | 159.610 | 151.328 | 151.111 | 143.538 | 143.269 |
| $3d_{3/2}4p_{1/2}(1)$ | $3d_{3/2}4d_{5/2}(1)$ | 169.949 | | 160.632 | | 152.045 | | 144.092 | |
| $3d_{3/2}4p_{1/2}(2)$ | $3d_{3/2}4d_{3/2}(3)$ | 170.502 | 170.677 | 161.223 | 161.346 | 152.703 | 152.771 | 144.848 | 144.855 |
| $3d_{5/2}4p_{1/2}(3)$ | $3d_{5/2}4d_{3/2}(2)$ | 171.111 | | 161.693 | | 153.056 | | 145.111 | |
| $3d_{3/2}4p_{1/2}(2)$ | $3d_{3/2}4d_{3/2}(1)$ | 171.911 | | 162.471 | | 153.816 | | 145.831 | |
| $3d_{5/2}4p_{1/2}(3)$ | $3d_{5/2}4d_{3/2}(4)$ | 171.963 | 171.798 | 162.529 | 162.323 | 153.873 | 153.624 | 145.906 | 145.602 |
| $\lambda_{expt}$ | | 171.987 | | | | | | | |
| $3d_{3/2}4p_{1/2}(1)$ | $3d_{3/2}4d_{3/2}(1)$ | 173.627 | | 164.275 | | 155.666 | | 147.708 | |
| $3d_{5/2}4p_{1/2}(2)$ | $3d_{5/2}4d_{3/2}(1)$ | 176.856 | 176.901 | 167.088 | 167.049 | 158.124 | 157.999 | 149.855 | 149.651 |
| $3d_{5/2}4p_{3/2}(2)$ | $3d_{3/2}4d_{3/2}(3)$ | 178.785 | 178.710 | 169.418 | 169.318 | 160.837 | 160.710 | 152.954 | 152.784 |
| $3d_{3/2}4p_{1/2}(2)$ | $3d_{5/2}4d_{5/2}(3)$ | 179.454 | 179.363 | 170.324 | 170.145 | 161.969 | 161.683 | 154.264 | 153.878 |
| $3d_{3/2}4p_{1/2}(1)$ | $3d_{5/2}4d_{5/2}(2)$ | 179.900 | 179.848 | 170.950 | 170.771 | 162.720 | 162.415 | 155.125 | 154.688 |
| $3d_{5/2}4p_{3/2}(4)$ | $3d_{5/2}4d_{5/2}(4)$ | 182.780 | 182.397 | 174.019 | 173.560 | 166.017 | 165.475 | 158.669 | 158.042 |
| $3d_{5/2}4p_{3/2}(4)$ | $3d_{5/2}4d_{5/2}(3)$ | 184.826 | | 175.988 | | 167.920 | | 160.508 | |
| $3d_{3/2}4p_{3/2}(0)$ | $3d_{3/2}4d_{5/2}(1)$ | 185.096 | 184.774 | 176.397 | 176.006 | 168.447 | 167.969 | 161.132 | 160.567 |
| $3d_{3/2}4p_{3/2}(3)$ | $3d_{3/2}4d_{5/2}(3)$ | 184.977 | 184.743 | 176.117 | 175.810 | 168.025 | 187.633 | 160.598 | 160.114 |
| $3d_{3/2}4p_{3/2}(3)$ | $3d_{3/2}4d_{5/2}(2)$ | 187.103 | | 178.163 | | 169.987 | | 162.482 | |
| $3d_{5/2}4p_{3/2}(2)$ | $3d_{5/2}4d_{5/2}(2)$ | 187.111 | 186.658 | 178.024 | 177.495 | 169.734 | 169.120 | 162.136 | 161.430 |
| $3d_{3/2}4p_{3/2}(3)$ | $3d_{3/2}4d_{3/2}(2)$ | 187.991 | | 179.369 | | 171.530 | | 164.352 | |
| $3d_{3/2}4p_{3/2}(1)$ | $3d_{3/2}4d_{5/2}(2)$ | 188.076 | 187.645 | 178.968 | 178.480 | 170.655 | 170.096 | 163.023 | 162.391 |
| $3d_{5/2}4p_{3/2}(4)$ | $3d_{5/2}4d_{3/2}(3)$ | 188.481 | | 179.808 | | 171.924 | | 164.697 | |
| $3d_{5/2}4p_{3/2}(1)$ | $3d_{5/2}4d_{5/2}(2)$ | 188.489 | | 179.256 | | 170.841 | | 163.146 | |
| $3d_{5/2}4p_{3/2}(2)$ | $3d_{5/2}4d_{5/2}(3)$ | 188.653 | 188.255 | 179.496 | 179.034 | 171.149 | 170.603 | 163.491 | 162.857 |
| $\lambda_{expt}$ | | 188.590 | | | | | | | |
| $3d_{3/2}4p_{3/2}(2)$ | $3d_{3/2}4d_{5/2}(3)$ | 188.637 | 188.329 | 179.560 | 179.180 | 171.265 | 170.809 | 163.656 | 163.112 |
| $3d_{3/2}4p_{3/2}(1)$ | $3d_{3/2}4d_{3/2}(2)$ | 188.973 | 188.872 | 180.185 | 180.060 | 172.210 | 172.027 | 164.905 | 164.669 |
| $3d_{3/2}4p_{3/2}(3)$ | $3d_{3/2}4d_{5/2}(4)$ | 189.224 | 188.817 | 180.164 | 179.687 | 171.892 | 171.328 | 164.299 | 163.638 |
| $\lambda_{expt}$ | | 189.092 | | 180.218 | | | | | |
| $3d_{5/2}4p_{3/2}(4)$ | $3d_{5/2}4d_{5/2}(5)$ | 189.319 | 188.901 | 180.263 | 179.768 | 171.989 | 171.407 | 164.388 | 163.716 |
| $\lambda_{expt}$ | | 189.315 | | 180.218 | | 172.055 | | | |
| $3d_{5/2}4p_{3/2}(3)$ | $3d_{5/2}4d_{5/2}(4)$ | 189.279 | 188.858 | 180.156 | 179.665 | 171.827 | 171.254 | 164.180 | 163.524 |
| $\lambda_{expt}$ | | 189.230 | | 180.218 | | | | | |
| $3d_{3/2}4p_{3/2}(0)$ | $3d_{3/2}4d_{3/2}(1)$ | 189.468 | | 180.800 | | 172.903 | | 165.667 | |
| $3d_{5/2}4p_{3/2}(3)$ | $3d_{5/2}4d_{5/2}(2)$ | 189.887 | | 180.750 | | 172.406 | | 164.750 | |
| $3d_{3/2}4p_{3/2}(2)$ | $3d_{3/2}4d_{5/2}(2)$ | 190.849 | 190.426 | 181.687 | 181.196 | 173.304 | 172.745 | 165.613 | 164.791 |
| $3d_{5/2}4p_{3/2}(3)$ | $3d_{5/2}4d_{5/2}(3)$ | 191.475 | 191.082 | 182.268 | 181.804 | 173.866 | 173.312 | 166.150 | 165.504 |
| $3d_{3/2}4p_{3/2}(2)$ | $3d_{3/2}4d_{3/2}(2)$ | 191.773 | | 182.941 | | 174.907 | | 167.556 | |
| $3d_{5/2}4p_{3/2}(4)$ | $3d_{5/2}4d_{3/2}(4)$ | 192.413 | | 183.619 | | 175.609 | | 168.273 | |
| $3d_{5/2}4p_{3/2}(2)$ | $3d_{5/2}4d_{3/2}(3)$ | 192.462 | | 183.472 | | 175.311 | | 167.839 | |
| $3d_{3/2}4p_{3/2}(1)$ | $3d_{3/2}4d_{5/2}(1)$ | 192.885 | | 183.627 | | 175.190 | | 167.426 | |
| $3d_{5/2}4p_{3/2}(2)$ | $3d_{5/2}4d_{5/2}(1)$ | 194.060 | | 184.721 | | 176.199 | | 168.379 | |
| $3d_{3/2}4p_{3/2}(3)$ | $3d_{3/2}4d_{3/2}(3)$ | 194.724 | | 185.851 | | 177.760 | | 170.362 | |
| $3d_{5/2}4p_{3/2}(3)$ | $3d_{5/2}4d_{3/2}(3)$ | 195.400 | 195.302 | 186.369 | 186.240 | 178.163 | 177.973 | 170.643 | 170.401 |

$3d_{3/2}4s_{1/2}(1)$-$3d_{5/2}4p_{3/2}(2)$ in $Sn^{22+}$], where the disagreement is about 0.2%. Since the relativistic MBPT calculations are more accurate for high-$Z$ ions, we conclude that the MBPT method provides accurate wavelengths for $3d_{j_1}4s_{1/2}(J)$-$3d_{j_2}4p_j(J')$ for ions with $Z>50$.

Only several lines for $3d_{j_1}4p_{j_2}(J)$-$3d_{j_3}4d_{j_4}(J')$ transitions were observed and identified by Churilov *et al.* [15] in Ni-like ions with $Z=47$–50. These data, together with our MBPT data and predicted theoretical data [16], are presented in Table X. The GLS label is used for data from Ref. [16], since they were determined in generalized least-squares fits using all known levels in the Ni sequence. As can be seen from Table X, our MBPT data $\lambda_{\mathrm{MBPT}}$ are in better agreement with experimental data $\lambda_{\mathrm{expt}}$ than with predicted data $\lambda_{\mathrm{GLS}}$.

## V. OSCILLATOR STRENGTHS, FOR DIPOLE TRANSITIONS TO THE GROUND STATE

As mentioned previously, line strengths, oscillator strengths, and transition rates for dipole transitions between odd-parity states with $J=1$ and the ground state are calculated in Ni-like ions with nuclear charges ranging from $Z=29$ to 100. Results are obtained in both length and velocity forms, but only length-form results are tabulated, since length-velocity differences are less than 1% for most cases.

In Figs. 2–6, we present the $Z$ dependence of oscillator strengths of transitions from $J=1$ excited states to the ground states. The sharp features in the curves shown in these figures can be explained in many cases by the strong mixing of states inside the odd-parity complex with $J=1$. In Fig. 2, the double cusp in the interval $Z=57$–59 is due to mixing of the $3d_{5/2}4f_{5/2}(1)$ and $3d_{5/2}4f_{7/2}(1)$ states. The mixing of the $3d_{5/2}4f_{7/2}(1)$ and $3d_{3/2}4f_{5/2}(1)$ states in the $Z=55$–56 range gives a singularity in the curve with the $3d_{5/2}4f_{7/2}(1)$ label. The mixing of the $3d_{3/2}4f_{5/2}(1)$ and $3p_{3/2}4s_{1/2}(1)$ states in the $Z=49$–50 range gives a singularity in the curve with the $3d_{3/2}4f_{5/2}(1)$ label. The deep minimum in the curve with the $3d_{3/2}4p_{1/2}(1)$ label in the $Z=43$–44 range can be explained by mixing of the $3d_{3/2}4p_{1/2}(1)$ and $3d_{5/2}4p_{3/2}(1)$ states. Most of the remaining singularities in Figs. 2–6 can be explained in a similar way.

These singularities are a consequence of coupling between states governed by the first-order mixing coefficients $C_1^N[av(J)]$ in Eq. (2.17). Comparison with the MCDF oscillator strengths given in Ref. [14] confirms this conclusion. However, some of the singularities are caused by second-order uncoupled matrix elements. As can be seen from the expression for $Z_K^{(\mathrm{RPA})}$ [Eq. (2.14)], the dominator of one term is $\epsilon_{bv}-\epsilon_{na}$. When $v=4d_{5/2}$, $a=3p_{3/2}$, $n=5p_{3/2}$, and $b=3d_{5/2}$, the sign of the denominator changes sign in the interval $Z=57$–58, and the denominator becomes very small for $Z=57$. A similar situation occurs for other cases: $\epsilon_{4p_{3/2}}-\epsilon_{3s_{1/2}}+\epsilon_{3d_{5/2}}-\epsilon_{5f_{7/2}}$ changes signs in the interval $Z=66$–67, and so forth. In these cases, the contribution of the term with these small denominators becomes much larger than other contributions, leading to new singularities in the $Z$ dependence of the oscillator strengths. We removed some of these singularities by increasing our model space to include $3d_jnp_{j'}$ and $3d_jnf_{j'}$ states with $n=5$ and 6, and simultaneously removing the states from the sum over $n$ in the expression for $Z_K^{(\mathrm{RPA})}$ in Eq. (2.14).

As can be seen from Figs. 3 and 4, some small singularities still remain for $3p_j4s_{1/2}(1)$ states in the $Z=29$–35 range, and $3p_j4d_{j'}(1)$ in the $Z=29$–45 range. These $3p_j4s_{1/2}(1)$ and $3p_j4d_{j'}(1)$ states are autoionizing for the $3d_j$-hole threshold in the $Z=29$–35 and 29–40 ranges. In this case, the singularity is in the positive part of the spectra in the sum over $n$ in Eq. (2.14) for $Z_K^{(\mathrm{RPA})}$. Our conclusion concerning the importance of autoionizing states in low-$Z$ Ni-like ions for calculations of the oscillator strengths can be extended to other atomic data.

## VI. CONCLUSION

In summary, a systematic second-order MBPT study of excitation energies of the 106 $3l$-$4l'$ hole-particle states of Ni-like ions was presented. Theoretical wavelengths in the x-ray spectra of Ni-like ions $Ag^{19+}-Pb^{54+}$ differ from existing experimental wavelength data at the level 0.01–0.1 %. Wavelengths of $3l_14l_2(J)-3l_34l_4(J)$ transitions differ from existing experimental wavelengths for intermediate values of $Z$ at the level 0.07%. These data provide a smooth theoretical reference for line identification.

Also presented is a systematic second-order relativistic MBPT study of reduced matrix elements and oscillator strengths for dipole transitions into the ground state in Ni-like ions, with nuclear charges ranging from $Z=29$ to 100. The retarded dipole matrix elements include correlation corrections from Coulomb and Breit interactions. Both length and velocity forms of the matrix elements were evaluated, and small differences, caused by the nonlocality of the starting HF potential, were found between the two forms. Second-order MBPT transition energies were used to evaluate oscillator strengths. The importance of autoionizing states for calculations of the oscillator strengths in low-$Z$ Ni ions was found and discussed. We believe that our results will be useful in analyzing existing experimental data and in planning new experiments.

## ACKNOWLEDGMENTS

The work of W.R.J. was supported in part by National Science Foundation Grant No. PHY-99-70666. U.I.S. acknowledges partial support by Grant No. B503968 from Lawrence Livermore National Laboratory. The work of J.R.A. was performed under the auspices of the U.S. Department of Energy by the University of California, Lawrence Livermore National Laboratory under Contract No. W-7405-Eng-48.

[1] E. Avgoustoglou, W. R. Johnson, D. R. Plante, J. Sapirstein, S. Sheinerman, and S. A. Blundell, Phys. Rev. A **46**, 5478 (1992).
[2] E. Avgoustoglou, W. R. Johnson, Z. W. Liu, and J. Sapirstein, Phys. Rev. A **51**, 1196 (1995).
[3] E. Avgoustoglou and Z. W. Liu, Phys. Rev. A **54**, 1351 (1996).
[4] E. N. Avgoustoglou and D. R. Beck, Phys. Rev. A **57**, 4286 (1998).
[5] J. H. Scofield and B. J. MacGowan, Phys. Scr. **46**, 361 (1992).
[6] M. H. Chen and A. L. Osterheld, Phys. Rev. A **52**, 3790 (1995).
[7] Y. Li, J. Nilsen, J. Dunn, A. L. Osterheld, A. Ryabtsev, and S. Churilov, Phys. Rev. A **58**, R2668 (1998).
[8] H. Daido, S. Ninomiya, M. Takagi, Y. Kato, and F. Koike, J. Opt. Soc. Am. B **16**, 296 (1999).
[9] J. Nilsen, J. Dunn, A. L. Osterheld, and Y. Li, Phys. Rev. A **60**, R2677 (1999).
[10] R. Doron, M. Fraenkel, P. Mandelbaum, A. Zigler, and J. J. Schwob, Phys. Scr. **58**, 19 (1998).
[11] A. Zigler, P. Mandelbaum, J. J. Schwob, and D. Mitnik, Phys. Scr. **50**, 61 (1994).
[12] M. Busquet, D. Pain, J. Bauche, and E. Luc-Koenig, Phys. Scr. **31**, 137 (1985).
[13] M. Klapisch, J. J. Schwob, M. Fraenkel, and J. Oreg, J. Opt. Soc. Am. **61**, 148 (1977).
[14] P. Quinet and E. Biémont, Phys. Scr. **43**, 150 (1991), and references therein.
[15] S. S. Churilov, A. N. Ryabtsev, and J.-F. Wyart, Phys. Scr. **38**, 326 (1988).
[16] J.-F. Wyart, Phys. Scr. **36**, 234 (1987).
[17] M. S. Safronova, W. R. Johnson, and U. I. Safronova, Phys. Rev. A **53**, 4036 (1996).
[18] U. I. Safronova, W. R. Johnson, M. S. Safronova, and A. Derevianko, Phys. Scr. **59**, 286 (1999).
[19] M. H. Chen, K. T. Cheng, and W. R. Johnson, Phys. Rev. A **47**, 3692 (1993).
[20] W. R. Johnson, S. A. Blundell, and J. Sapirstein, Phys. Rev. A **37**, 2764 (1988).
[21] L. W. Fullerton and G. A. Rinker, Jr., Phys. Rev. A **13**, 1283 (1976).
[22] P. J. Mohr, Ann. Phys. (N.Y.) **88**, 26 (1974); **88**, 52 (1974); Phys. Rev. Lett. **34**, 1050 (1975).
[23] W. R. Johnson, D. R. Plante, and J. Sapirstein, Adv. At., Mol., Opt. Phys. **35**, 255 (1995).